A Density Functional, Infrared Linear Dichroism, and Normal Coordinate Study of Phenol and its Deuterated Derivatives: Revised Interpretation of the Vibrational Spectra

Gábor Keresztury*,†

Central Research Institute for Chemistry, Hungarian Academy of Sciences, H-1525 Budapest, P.O. Box 17, Hungary

Ferenc Billes‡ and Miklós Kubinyi§

Department of Physical Chemistry, Technical University of Budapest, H-1521 Budapest, Budafoki út 8, Hungary

Tom Sundius||

Department of Physics, University of Helsinki, P.O. Box 9, FIN-00014, Helsinki, Finland

Received: August 7, 1997; In Final Form: November 6, 1997

The assignment of the vibrational spectra of phenol has been reexamined on the basis of Raman and new IR measurements and theoretical analysis of the normal modes of vibrations in the electronic ground state. The infrared spectra of C_6H_5OH, C_6D_5OD, and C_6D_5OH have been studied in solution and vapor phases, as well as has the Raman spectra in solutions. New experimental data were obtained from infrared linear dichroism (IR-LD) studies of phenol aligned in uniaxially oriented nematic liquid crystal solution. The measured dichroic ratios and orientation factors indicate an effective C_s symmetry of the molecule with coplanar orientation of OH bond with the benzene ring and supply unique information on the extent of symmetry lowering of benzene normal modes. The fundamental vibrational frequencies, force constants, and dipole derivatives have been calculated by ab initio quantum chemical methods applying the B3P86 density functional approximation with 6-311G** basis set. The force field optimized by means of a least-squares scaling procedure for phenol-d_0 (using six scale factors) was used to calculate the frequencies (with a mean deviation from the observed values less than 1%), normal modes, potential energy distributions, transition moment vectors, and IR intensities for phenol-d_0, -d_1, -d_5, and -d_6 isotopomers. Compared to the deviations between the calculated and observed absorption intensities, a more satisfactory correlation was found between the calculated and experimentally determined *vibrational transition moment directions*. The results indicate unanimously that the perturbation of the normal modes of benzene by the asymmetric hydroxyl substituent is so great that the previous practice of assigning the normal vibrations of phenol to those of benzene or even to C_{2v} symmetry species is not justified.

I. Introduction

A number of articles were published during the last 40 years on the molecular structure[1−6] and vibrational spectra[7−17] of phenol reporting the results of both experimental and theoretical studies. In this paper we are going to present a reassessment of the vibrational assignment of the IR and Raman spectra of phenol on the basis of new experimental data and high-level quantum chemical force field and normal coordinate calculations fully supporting each other. Our interpretation is aimed at eliminating some of the contradictions encountered in earlier works.

The structure of phenol molecule in the ground electronic state (Figure 1) has been studied by several authors. The experimental geometry of the free molecule has been determined by Larsen[1] on the basis of the microwave spectra of six isotopomers and by Portalone et al.[2] by means of electron diffraction. Konschin[3] calculated the optimized molecular structure with ab initio HF/STO-3G method, Puebla and Ha[4] used the HF/4-31G approximation, while Bock et al.[5] applied the ab initio HF method with 6-31G and 6-31G* basis sets. Later Bock et al.[6] calculated the equilibrium geometry using MP2 perturbation with 6-31G* basis set. The structural parameters determined in the papers cited above are collected in Table 1 (the numbering of atoms used is given in Figure 1).

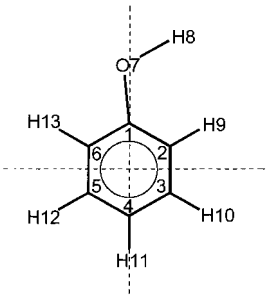

Figure 1. Numbering of the atoms in phenol molecule.

The vibrational spectra of phenol have also been investigated quite extensively. Concerning the assignment of fundamental

† E-mail: kergabor@cric.chemres.hu.
‡ E-mail: billes@ch.bme.hu.
§ E-mail: kubinyi@ch.bme.hu.
|| E-mail: sundius@phcu.helsinki.fi.

S1089-5639(97)02585-1 CCC: $15.00
Published on Web 02/03/1998

TABLE 1: Experimental and Calculated Structural Parameters of Phenol Molecule

	experimental		Hartree−Fock					
parameter[a]	MW[b]	ED[c]	STO3G[d]	4-31G[e]	6-31G[f]	6-31G*[f]	MP2 (6-31G*[g])	DFT/B3P86 (6-311G**[h])
C1−C2	1.391	1.399	1.397	1.381	1.385	1.385	1.395	1.393
C2−C3	1.394	1.399	1.386	1.385	1.389	1.387	1.395	1.390
C3−C4	1.395	1.399	1.390	1.381	1.385	1.382	1.393	1.389
C4−C5	1.395	1.399	1.384	1.387	1.390	1.388	1.396	1.392
C5−C6	1.392	1.399	1.382	1.379	1.383	1.381	1.392	1.387
C6−C1	1.391	1.399	1.392	1.383	1.386	1.388	1.396	1.393
C2−H9	1.086	1.083	1.082	1.073	1.074	1.077	1.089	1.087
C3−H10	1.084	1.083	1.083	1.072	1.073	1.075	1.087	1.084
C4−H11	1.080	1.083	1.082	1.071	1.072	1.074	1.086	1.083
C5−H12	1.084	1.083	1.083	1.072	1.072	1.075	1.087	1.085
C6−H13	1.081	1.083	1.082	1.069	1.070	1.074	1.086	1.083
C1−O7	1.375	1.381	1.395	1.374	1.377	1.352	1.374	1.360
O7−H8	0.957	0.958	0.989	0.950	0.949	0.947	0.973	0.961
C6C1C2	120.9	121.6	119.8	120.4	120.6	120.1	120.3	119.9
C1C2C3	119.4	118.8	119.9	119.6	119.4	119.6	119.7	119.9
C2C3C4	120.5	120.6	120.5	120.5	120.4	120.5	120.5	120.5
C3C4C5	119.2	119.7	119.4	119.4	119.4	119.2	119.4	119.3
C4C5C6	120.8	120.6	120.8	120.7	120.6	120.7	120.6	120.8
C5C6C1	119.2	118.8	119.6	119.6	119.4	119.5	119.6	119.7
C1C2H9	120.0		120.4	120.2	120.3	120.0	120.1	119.9
C2C3H10	119.5		120.3	119.4	119.5	119.4	119.2	119.3
C3C4H11	120.3		120.4	120.3	120.3	120.4	120.3	120.4
C4C5H12	119.8		119.8	119.9	119.9	119.9	120.1	120.0
C5C6H13	121.6		121.3	121.7	121.9	121.6	121.6	121.6
C6C1O7	117.0	117.2	117.7	117.0	116.8	117.3	116.9	117.6
C1O7H8	108.8	106.4	104.9	114.8	114.7	110.7	108.4	108.8

[a] Distances in angstroms, angles in degrees. [b] Reference 1. [c] Reference 2. [d] Reference 3. [e] Reference 4. [f] Reference 5. [g] Reference 6. [h] This work; E(RB+HF-VWN+P86) = −308.445 775 970 hartree.

vibrations, the results of earlier works are collected and compared in Table 2. An early paper by Mecke and Rossmy[7] reported the infrared spectra of phenol and its OD isotopomer including the study of solvent effects. Later Evans[8] published a study of the infrared (in vapor, solution, neat liquid, and solid phase) and Raman spectra (including depolarization data) of C_6H_5OH and C_6H_5OD, and proposed a complete vibrational assignment for these compounds. Green[9] published an independent assignment of the vibrational spectra of the same compounds. Bist et al.[10] studied the vibrations of C_6H_5OH, C_6H_5OD, and C_6D_5OH, and in the assignment of the vibrational spectra they used also the vibronic vapor spectra of these isotopomers. In his often-cited book Varsányi[11] assigned, among 700 molecules, the IR spectra of phenol and O-deuterated phenol on the basis of systematic comparison of the spectra of a great number of "mono-light-substituted" benzenes. Larsen and Nicolaisen[12] and later Hutt and Butcher[13] have investigated the far-infrared spectrum of phenol, while Wilson et al.[14] measured and interpreted the Raman vapor spectrum.

Normal coordinate calculations have been performed on phenol by Kovner et al.[15] using the classical GF-matrix method. Sarin et al.[16] used semiempirical formulas to calculate the PR separations and relative Q-branch intensities in the vapor spectrum, while Puebla and Ha[4] applied the ab initio HF/4-31G method for the calculation of vibrational frequencies but published only a few calculated frequencies. In our earlier work,[17] we applied the semiempirical CNDO/2 method with a subsequent scaling of the calculated force constants to achieve a better frequency fit. The intensities and polarization properties of the IR absorption bands have not been studied yet.

Most of the earlier assignments reviewed in Table 2 were based on comparison of phenol normal modes to those of benzene, and the fundamentals were designated using the accepted notation of benzene normal modes[11] or were assigned to the symmetry species of the hypothetical C_{2v} point group. Concerning the description of normal modes and the band assignments, the following main differences can be noted.

(**i**) While most of the authors regarded the molecule as planar, Green[9] accepted a model in which the plane of the COH group was perpendicular to the benzene ring.

(**ii**) Bist et al.[10] and Wilson et al.[14] used a choice of axes different from that of Evans[8] and Green[8] when adopting C_{2v} symmetry which led to different notation of the symmetry species.

(**iii**) Although the set of frequencies accepted by the different authors as fundamentals are more or less the same, there are genuine differences and contradictory assignments as well reflected by the labels corresponding to the normal modes of benzene.[11] It is particularly problematic to distinguish between the normal modes of vibrations within certain groups of vibrations, namely, 2, 20a and 20b; 7a, 7b and 13; 8a, and 8b; 15, 18a, and 18b; 1, 10a and 12a; and 10b and 11. Since the normal modes within these groups are very close in character, it is hard to identify them with benzene normal modes, especially under the conditions of low symmetry when they are more or less distorted.

(**iv**) The band at about 820 cm^{-1} was assigned by some authors to an in-plane motion[8−9,11] while others assigned it to an out-of-plane mode.[10,17] The reverse alternative assignments were given to a nearby band at about 810 cm^{-1}.

With the exception of our previous paper,[17] earlier descriptions of the fundamental vibrations of phenol were either limited to the indication of a single type of internal coordinate dominating in the normal mode and/or given in terms of the accepted numbering of the "corresponding" benzene normal modes. To the best of our knowledge, the only assignment based on potential energy distribution has been reported by us.[17] In that work, however, we applied the semiempirical CNDO/2 method, whereas these days far superior quantum mechanical approximations are available. A revision of the assignment of

TABLE 2: Earlier Assignments of Fundamental Vibrations of the Phenol Molecule[a]

Evans[b]		Green[c]		Bist[d]	
ν_i^{obs}	assignment	ν_i^{obs}	assignment	ν_i^{obs}	assignment
3610	νOH			3656	νOH
3074	νCH, B1	3091	νCH, A″, B1, 20b	3087	νCH, A1, 20a
3061	νCH, A1	3085	νCH, A′, A1, 20a	3070	νCH, B2, 20b
3052	νCH, B1	3076	νCH, A′, A1, 2	3063	νCH, A1, 2
3046	νCH, B1	3044	νCH, A′, A1, 13	3049	νCH, B2, 7b
3021	νCH, A1	3030	νCH, A″, B1, 7b	3027	νCH, A1, 13
1608	νrg, A1	1604	νCC, A′, A1, 8a	1610	νCC, B2, 8b
1600	νrg, B1	1596	νCC, A″, B1, 8b	1603	νCC, A1, 8a
1502	νrg, A1	1497	νCC, A′, A1, 19a	1501	νCC, A1, 19a
1473	νrg, B1	1465	νCC, A″, B1, 19b	1472	νCC, B2, 19b
		1333	νCC, A″, B1, 14	1343	νCC, B2, 14
		1313	βCH, A″, B1, 3		
1290	βCH, B1			1277[j]	βCH, B2, 3
1259	X-sensor, A1	1259	X-sensor, A′, A1, 7a	1261	νCO, A1, 7a
1228	βOH + νrg			1176	βOH
1167	βCH, A1	1167	βCH, A′, A1, 9a	1168	βCH, A1, 9a
1151	βCH, B1	1145	βCH, A″, B1, 9b	1150	βCH, B2, 9b
1070	βCH, B1	1071	βCH, A″, B1, 15	1070	βCH, B2, 15
1026	βCH, A1	1026	βCH, A′, A1, 18a	1025	βCH, A1, 18a
1000	βrg, A1	999	rg, A′, A1, 1	999	rg, A1, 1
972	γCH, B2	978	γCH, A″, B2, 5	995[j]	γCH, A2, 17a
958	γCH, A2	958	γCH, A″, A2, 17a	973	γCH, B1, 5
883	γCH, B2	881	γCH, A′, B2, 17b	881	γCH, B1, 17b
829	γCH, A2	825	γCH, A″, A2, 10a	823	X-sensor, A1, 12
814	X-sensor, A1	810	X-sensor, A′, A1, 12a	817[j]	γCH, A2, 10a
753	γCH, B2	749	γCH, A′, B2, 10b	751	γCH, B1, 10b
691	γrg, B2	688	γCC, A′, B2, 4	686	γCC, B1, 4
619	βrg, B1	617	γCC, A″, B1,6b	619	rg, B2, 6b
530	X-sensor, A1	526	X-sensor, A′, A1, 6a		
508	X-sensor, B2	500	X-sensor, A′, B2, 16b	503	X-sensor, B1, 16b
415	γrg, A2	408	γCC, A″, A2, 16a	409[j]	γCC, A2, 16a
404	X-sensor, B1	408	X-sensor, A″, A2, 18b	403	X-sensor, B2, 18b
				309	τOH
242	X-sensor, B2	241	X-sensor, A′, B2, 11	244	X-sensor, B1, 11

Varsányi[e]		Wilson[f]		Sarin[g]		Kovner[h]	
ν_i^{obs}	assignment	ν_i^{obs}	assignment	ν_i^{obs}	type	ν_i^{obs}	ν_i^{calcd}
3623	νOH	3656	νOH	3656	A[k]	3650	3653
3091	20a					3071	3075
3076	2	3073	A1, 2			3061	3070
3048	20b					3052	3061
3044	7b					3046	3054
3030	7a					3021	3045
1604	8a	1612	B2, 8b			1603	1624
1596	8b	1602	A1, 8a			1597	1610
1497	19a	1504	A1, 19a	1501	A	1502	1504
1465	19b	1470	B2, 19b	1471	B[k]	1474	1477
1333−1376	14	1388	B2, 14	1344	B[k]	1370	1374
1313	3					1292	1312
		1285	B2, 3			1252	1239
1259	13	1264	A1, 7a			1230	1233
1180−1235	βOH	1196					
1167	9a	1168	A1, 9a			1170	1174
1145	9b	1149	B2, 9b			1155	1154
1071	18b			1070	B	1072	1070
1026	18a	1025	A1, 18a	1026	A[k]	1025	1017
999	12	999	A1, 1			1000	1001
978	5						
958	17a						
881	17b			881	C		
825	10a	824	A1, 12				
810	1					814	773
749	11			751	C		
688	4			686	C		
617	6b					620	608
526	6a	528	A1, 6a			530	498
500	16b						
410	16a						
408	15			403	B[k]		
300	γOH			310	C	398	415
241	10b	235	B1, 11				

TABLE 2 (continued)

Kubinyi[i]		
ν_i^{obs}	ν_i^{calcd}	assignment (PED %)
3610	3600	A′, νOH(100)
3074	3063	A′, νCH(99)
3061	3061	A′, νCH(99)
3052	3054	A′, νCH(99)
3046	3045	A′, νCH(100)
3021	3038	A′, νCH(100)
1608	1628	A′, νCC(58), βCH(20), βCC((13)
1600	1613	A′, νCC(63), βCH(13)
1502	1492	A′, βCH(55), νCC(34)
1473	1469	A′, βCH(48), νCC(30), βOH(15)
1344	1363	A′, βCH(72), βOH(21)
1290	1281	A′, βCH(39), νCC(36), βOH(11)
1259	1269	A′, νCO(37), νCC(23), βCH(23)
1179	1179	A′, νCC(38), βOH(31), βCH(29)
1167	1162	A′, βCH(74), νCC(25)
1151	1155	A′, βCH(58), νCC(38)
1070	1054	A′, νCC(58), βCH(35)
1026	1007	A′, νCC(72), βCH(21)
1000	985	A′, βCC(61), νCC(38)
972	965	A″, γCH(122), γCC(-22)
958	954	A″, γCH(114), γCC(-14)
	885	A″, γCH(102), γCC(-10)
829	831	A″, γCH(100)
814	800	A′, νCC(40), βCC(34), νCO(23)
753	750	A″, γCC(53),γCH(27)
691	701	A″, γCC(54), γCH(47)
619	634	A′, βCC(80), νCC(15)
530	519	A′, βCC(73), νCO(13), νCC(11)
508	492	A″, γCC(53), γCO(43)
415	421	A″, γCC(112), γCH(-14)
310	309	A″, τOH(98)
404	402	A′, βCO(82)
242	229	A″, γCC(71), γCO(33)

[a] Frequencies in cm^{-1}: ν, stretch; β, bend; γ, oop. bend; τ, torsion; X, substituent; rg, ring. [b] Reference 8. [c] Reference 9. [d] Reference 10. [e] Reference 11. [f] Reference 14, Raman vapor spectrum. [g] Reference 15. [h] Reference 14. [i] Reference 16, CNDO/2 calculations. [j] From UV vapor spectrum. [k] Hybrid band.

the vibrational spectra of phenol is therefore desirable utilizing a force field derived from a modern post-Hartree−Fock calculation done with sufficiently large basis set.

In what follows we present the results of such a calculation together with new experimental evidence obtained from linear dichroism (LD) measurements that has prompted us to discard the C_{2v} symmetry species for classification of phenol vibrations and give a revised assignment more consistent with all available data.

II. Experimental Section

C_6H_5OH and C_6D_5OD were purchased from Aldrich and used without further purification, while C_6D_5OH was obtained by recrystallization of C_6D_5OD from water.

The FT-IR spectra of phenol, C_6D_5OH, and hexadeuteriophenol were measured in vapor phase and in CCl_4 and CS_2 solutions. The spectra were recorded on a Nicolet Magna 750 FT-IR spectrometer at 1 and 2 cm^{-1} resolution using a 0.016 mm KBr liquid cell for the solutions and a 1 m gas cell (Carl Zeiss Jena) for phenol vapors.

Raman spectra of phenol isotopomers were measured in CCl_4 and CS_2 solutions on a Nicolet FT-Raman Model 950 spectrometer at 2 cm^{-1} resolution using the 1064 nm line of a Nd:YAG laser for excitation.

Polarized IR spectra were measured with the sample aligned in uniaxially oriented nematic liquid crystal. A Perkin-Elmer Au/AgCl wire grid polarizer placed in front of the sample was used to generate linearly polarized radiation. The sample consisted of a 5% (m/m) solution of phenol in liquid crystal ZLI-1695 (Merck) filled into a 0.024 mm KBr liquid cell with specially pretreated windows.[18] The two absorbance spectra recorded with the electric vector of light oriented parallel and perpendicular to the director of the liquid crystal were used in a stepwise reduction process[19] to obtain the so-called reduced spectra and the dichroic ratios d_i of every band by successive interactive subtractions. The orientation factors and transition moment directions were calculated from the observed dichroic ratios using the formulas given by Michl and Thulstrup.[19]

In order to determine the positions and intensities of spectral bands more precisely, the overlapping bands in both IR and Raman spectra were resolved by curve fitting.

TABLE 3: Optimized Scale Factors for the Phenol Force Field Obtained from the DFT/B3P86/6-311G Calculation**

type of coordinate[a]	scale factor
CH, CC, and CO stretching	0.9135
CCH and CCO bending	0.9860
CCC bending	0.9675
OH stretching	0.8903
COH bending	0.9996
C−OH torsion	0.5930

[a] Force constants corresponding to coordinates not listed here were kept unscaled.

III. Computational Details

Ab initio QM calculations were performed applying the density functional theory with Becke's three-parameter functional, B3P86[20] and a large basis set, 6-311G**, by means of the Gaussian 92/DFT program package.[21]

First the vibrational force constants, harmonic vibrational frequencies, net atomic charges, the dipole moment, and its derivatives and the thermodynamic properties of *undeuterated phenol* were calculated. Our preliminary geometry optimizations done with simultaneous relaxation of all structural parameters led to a practically planar structure; thus, in the final optimization, the geometry was constrained to C_s symmetry and the perfectly planar optimized structure was used as an equilibrium reference geometry. The reference geometry and the corresponding Cartesian force constant matrix ($\mathbf{F}_x$) were taken as starting data in all further calculations. The $\mathbf{F}_x$ matrix was transformed into a nonredundant set of 33 suitable internal coordinates (the "natural coordinates") constructed according to the recommendations.[22] These coordinates include 13 bond stretches, 5 CH, 1 CO, 1 OH, and 3 ring in-plane bending coordinates; 1 OH and 3 ring out-of-plane torsions, and 5 CH and 1 CO out-of-plane bending coordinates.

The **F** matrix obtained was scaled using six empirical scaling factors to ensure a better fit of observed and calculated frequencies. The multiple scaling method of Fogarasi and Pulay[23] was used with a least-squares refinement of the scale factors, whereas the calculated vibrational frequencies of phenol-d_0 were fitted to the experimentally assigned normal frequencies. Six scale factors were used in all; their optimized values are given in Table 3. The same optimized (scaled) general valence force field was applied also for the frequency calculations of the three deuterated phenol isotopomers. In addition to the frequencies and vibrational eigenvectors, the potential energy distribution (PED) matrices, transition moment vectors, and relative absorption intensities were also calculated for characterization of the normal modes. These final calculations were also performed for C_6H_5OD, C_6D_5OH, and C_6D_5OD isotopomers.

TABLE 4: Measured and Calculated (DFT/B3P86/6-311G, Scaled Force Field) Vibrational Frequencies and Relative Absorption Intensities of C_6H_5OH Fundamentals**

	frequency (cm^{-1})		intensity (arbitrary units)		
i	measd[b]	calcd	measd[b]	calcd	potential energy distribution (%)
1	3655	3655	104.22	60.7	νOH(100)
2	3074	3073	0.35	4.2	νCH(99)
3	3061	3066	1.75	15.5	νCH(99)
4	3052	3053	4.29	15.7	νCH(99)
5	3046	3045	11.83	0.2	νCH(99)
6	3021	3025	1.93	13.7	νCH(99)
7	1609	1613	36.09	40.0	νCC(64), βCH(18), βCC(10)
8	1604	1601	62.90	47.3	νCC(66), βCH(16), βCC(9)
9	1501	1502	69.12	48.1	βCH(56), νCC(33), νCO(6)
10	1472	1476	42.92	39.5	βCH(52), νCC(33), βOH(8)
11	1361	1359	0.96	43.8	βCH(63), βOH(26), νCC(7)
12	1344	1328	17.52	6.0	νCC(63), βCH(33)
13	1261	1260	51.33	77.6	νCO(50) , νCC(19), βCH(17), βCC(10)
14	1197	1192	106.26	135.5	βOH(45), νCC(26), βCH(23)
15	1176	1170	10.34	7.4	βCH(75), νCC(24)
16	1150	1159	13.87	10.8	νCC(23), βCH(74)
17	1070	1069	12.18	12.7	νCC(55), βCH(38)
18	1026	1015	4.73	3.8	νCC(69), βCH(23), βCC(6)
19	999	986	3.68	4.0	βCC(61), νCC(37)
20	973	977	0.26	0.01	γCH(83), γCC(17)
21	956	955	0.18	0.1	γCH(88), γCC(12)
22	881	878	8.94	6.9	γCH(88), γCC(12)
23	(823)	811		0.04	γCH(99)
24	810	808	17.78	18.7	νCC(42), βCC(30), νCO(24)
25	752	755	74.81	67.4	γCH(65), γCO(27), γCC(7)
26	687	687	42.92	26.6	γCC(91), βCH(5)
27	618	620	0.61	0.4	βCC(82), νCC(11), νCO(5)
28	526	525	1.93	1.7	βCC(78), νCO(11), νCC(9)
29	503	512	20.5	13.8	γCC(49), γCO(45), γCH(6)
30	420	410	0	0.4	γCC(88), γCH(12)
31	410	402	8.23	9.9	βCO(79), νCC(8), βCC(8)
32	310[d]	307		111.2	τOH(97)
33	242[d]	228		1.8	γCC(87), γCO(13)

[a] Mean deviation in frequencies: 4.85 cm^{-1} (0.70%). [b] Vapor. [c] CCl_4 solution. [d] From ref 17.

The dipole derivatives (derivatives of the electric dipole moment with respect to the atomic coordinates) obtained from the DFT calculation were used to calculate the vibrational transition moments (i.e., the dipole derivatives with respect to the normal coordinates (corresponding to the scaled force field)). The directions of the calculated transition moment vectors were used, via comparison to the values determined experimentally from the IR linear dichroism measurements, to correct for the sign ambiguity of the latter values and to evaluate the extent of symmetry lowering of the normal modes.[24]

IV. Results and Discussion

A. Structural Parameters. The optimized structural parameters of phenol obtained from the DFT calculation using B3P86/6-311G** method are compared with the experimental data and earlier calculated values in Table 1 (last column) where the numbering of atoms is as given in Figure 1. Of the two experimental structure determinations the microwave measurement of Larsen[1] yielded more detailed results: he allowed individual values for all bond lengths and valence angles in the determination of the r_s structure. In contrast, Portalone et al.[2] in their electron diffraction work assumed equal lengths for the six C−C bonds as well as for the five C−H bonds and even the bond angles were constrained to C_{2v} symmetry of the ring. Nonetheless, the numerical values obtained by the two experimental methods are rather close; yet the microwave results do not justify the assumptions made in the electron diffraction work.

Regarding the ab initio HF calculated values, the STO-3G results[3] show the greatest deviations from the experimental ones. The other HF calculations done with larger basis sets[4−5] underestimate the C−C and C−H bond lengths but give good or acceptable values for the C−O and O−H distances; their optimum valence angles are also acceptable with the exception of the C−O−H angle that is overestimated.

Our DFT calculation shows the best overall agreement with the experimentally determined values, the results of the MP2 calculation[6] being almost equally good. Both methods produced slightly different values for the individual C−C and C−H bond lengths; the values are similar to those of the r_s structure, but their distribution around the ring is different. It is probably well founded to state that in the equilibrium structure the shape of the phenyl ring deviates slightly from a regular hexagon and it does not have even C_{2v} symmetry. The C1−O7 bond makes an angle of nearly 3° with the axis passing through the C1 and C4 atoms (see Figure 1). The C−O bond length is a little underestimated in the present calculation, while the O−H distance is in good accordance with the r_s one. There is an excellent agreement between our calculated values and the experimental r_s data for all valence angles.

In summary, one may conclude that our calculated structure provides a reliable starting point for the DFT/B3P86/6-311G** force field and frequency calculations.

B. Fundamental Vibrational Frequencies and Intermolecular Association. The primary aim of our infrared and Raman survey measurements was to check the correctness of the experimental frequency values that were used in earlier studies, with high-precision, up-to-date instrumentation. The results obtained for the four phenol isotopomers are in good

TABLE 5: Measured and Calculated (DFT/B3P86/ 6-311G, Scaled Force Field) Vibrational Fundamentals of C_6H_5OD[a]**

frequencies (cm^{-1})		
measd[b]	calcd	potential energy distribution (%)
3075	3073	νCH(99)
3062	3067	νCH(99)
3046	3054	νCH(99)
3040	3045	νCH(99)
3014	3026	νCH(99)
2670	2661	νOD(99)
1602	1609	νCC(64), βCH(21), βCC(10)
1597	1592	νCC(68), βCH(16), βCC(9)
1499	1498	βCH(59), νCC(33), νCO(6)
1463	1464	βCH(56), νCC(35), βOD(5)
1333	1334	βCH(80), νCC(14)
1305	1311	νCC(72), βCH(19)
1251	1255	νCO(52), νCC(18), βCH(16), βCC(12)
1169	1169	βCH(75), νCC(24)
1156	1160	βCH(76), νCC(23)
1078	1077	νCC(48), βCH(44)
1027	1013	νCC(66), βCH(23), βCC(9)
1001	989	βCC(57), νCC(40)
970	978	γCH(84), γCC(16)
962	956	γCH(88), γCC(12)
932	942	βOD(78), νCC(16)
880	878	γCH(78), γCC(11), γCO(9)
827	811	γCH(99)
808	802	νCC(41), νCO(30), βCC(30)
753	755	γCH(66), γCO(27), γCC(7)
690	686	γCC(92), γCH(4)
617	622	βCC(83), νCC(11), νCO(4)
528	522	βCC(76), νCC(9), νCO(11)
511	511	γCC(49), γCO(45), γCH(6)
416	406	γCC(88), γCH(12)
383	383	βCO(78), νCC(8), βCC(7)
241	241	τOD(47), γCC(44), γCO(10)
(232)	211	τOD(55), γCC(45)

[a] Mean deviation: 5.84 cm^{-1} (0.78%). [b] From ref 8.

TABLE 6: Measured and Calculated (DFT/B3P86/ 6-311G, Scaled Force Field) Vibrational Fundamentals of C_6D_5OH[a]**

frequencies (cm^{-1})		
measd	calcd	potential energy distribution (%)
3656	3655	νOH(100)
2294	2279	νCD(96)
2281	2271	νCD(96)
2262	2258	νCD(96)
2258	2248	νCD(97)
2249	2235	νCD(96)
1579	1581	νCC(74), βCC(9), βCD(9)
1567	1566	νCC(73), βCC(8), βCD(7)
1404	1403	νCC(46), βCD(17), βOH(16), νCO(13)
1372	1374	νCC(47), βCD(19), βOH(16), νCO(8)
1301	1318	βCC(85), βCD(7), βOH(6)
1204	1210	νCC(40), βOH(38), βCD(17)
1179	1184	νCO(38), νCC(26), βCD(18), βCC(12)
1021	1023	βCD(84), νCC(5), βCO(5), βOH(5)
960	948	βCC(62), νCC(33)
869	868	βCD(52), νCC(34), βCC(9)
837	843	βCD(82), νCC(15)
831	830	βCD(63), νCC(24), βCC(7)
813	812	βCD(78), νCC(9)
	801	γCD(92), γCC(5)
776	775	γCD(86), γCC(12)
756	758	γCD(60), γCO(36)
754	748	νCC(39), βCD(29), βCC(16), νCO(14)
636	634	γCD(95)
624	628	γCD(71), γCC(17), γCO(12)
594[b]	597	βCC(79), νCC(10)
550	552	γCC(64), γCD(33)
513	514	βCC(77), νCO(10), νCC(8)
430	435	γCD(39), γCC(31), γCO(29)
386[c]	385	βCO(76), νCC(9), βCC(8)
357	359	γCC(88), γCD(12)
307[c]	305	τOH(96)
232	214	γCC(85), γCO(10), γCD(5)

[a] Mean deviation: 5.00 cm^{-1} (0.66%). [b] Condensed phase value. [c] From ref 9b.

general agreement with the previously reported experimental data, with just a few minor deviations concerning the choice of fundamentals.

In order to be consistent with the DFT calculations where only isolated molecules were studied, we selected the vapor phase values of the fundamental frequencies for comparison wherever they could be located with certainty. They were typically 1−2 cm^{-1} higher than those reported by Evans.[8] The frequencies we assigned to fundamental vibrational transitions of the free molecules are listed in the first columns of Tables 4−7 for phenol-d_0, -d_1 (OD), -d_5 (OH), and -d_6, respectively. The solution data were used to check the number of bands in crowded spectral regions (where the interpretation of the rotational band structure in the vapor spectra posed greater difficulties) or as substitutes if the bands in the vapor spectrum were too weak to be observed (some γCH bands).

Phenol is prone to self-association which must be kept in mind when interpreting its condensed phase vibrational spectra. The spectral features significantly affected by H-bonding interactions are those of the OH-group: the OH stretching (νOH), bending (βOH), and out-of-plane bending, or torsional (τOH) bands. Our observations confirm the coexistence of free and different associated forms, their equilibrium being dependent on concentration. In Figure 2, the infrared spectrum of a 5% (m/m) solution of phenol in carbon tetrachloride is compared with that of a 1% solution (for easier comparison the intensity of the latter was multiplied by 5). The intensity of the monomer ν(OH) band at 3611 cm^{-1} decreases, while that of the down-shifted, broad band (3130−3540 cm^{-1}) belonging to the hydrogen-bonded OH groups increases with the concentration rapidly.

The influence of the environment on the position of the *monomer* ν(OH) band is shown in Figure 3. The νOH frequency of a monomeric phenol molecule is shifted toward lower frequencies in the order: vapor phase → CCl_4 solution → CS_2 solution. The relative permittivities of CCl_4 and CS_2 at 20 °C are 2.238 and 2.641, respectively, which suggests that the lowering of frequencies of the monomer νOH band in solution is due to the solvent polarity effect of the environment. A similar trend is observed for most of the other vibrations as well, although the shifts are usually much smaller: the CCl_4 solution frequencies are in general closer to the vapor phase values, while the CS_2 solution frequencies are 1−3 cm^{-1} lower.

At variance with previous investigators, we assign the OH bending mode of free phenol to a clearly observed Q-branch at 1198 cm^{-1}, a feature which may not have been resolved in earlier measurements. The broader band at 1218−1220 cm^{-1} in the solution spectra corresponds to the same mode of H-bonded OH-groups.

It is of interest to compare the IR spectra of phenol and hexadeuteriophenol. The fingerprint region of the CCl_4 solution spectra is shown in Figure 4 and the high frequency region in Figure 5. Note that simultaneously with the expected band shifts significant changes of band intensities occur, especially in the fingerprint region, that may be explained by altered intermolecular vibrational couplings.

TABLE 7: Measured and calculated (B/DFT3P86/6-311G, scaled force field) vibrational fundamentals of C_6D_5OD[a]**

frequencies (cm^{-1}) measd	calcd	potential energy distribution (%)
2655	2661	νOD(99)
2294	2279	νCD(96)
2286	2271	νCD(96)
2277	2258	νCD(96)
2256	2248	νCD(97)
2246	2235	νCD(96)
1585	1573	νCC(74), βCC(9), βCD(9)
1567	1557	νCC(76), βCC(7), βCD(6)
1391	1390	νCC(52), βCD(21), νCO(21)
1351	1345	νCC(61), βCD(24), βCO(7)
1292	1303	βCC(91)
1178	1184	νCO(40), νCC(26), βCD(18), βCC(13)
1056	1066	βCD(78), βOD(16)
957	948	βCC(60), νCC(34)
905	919	βOD(65), βCD(17), νCC(13)
874	868	βCD(55), νCC(33), βCC(8)
855	843	βCD(82), CC(15)
834	828	βCD(64), νCC(24), βCC(6)
811	812	βCD(77), νCC(20)
801	801	γCD(91), γCC(5)
786	775	γCD(88), γCC(10)
753	758	γCD(60), γCO(36)
750	744	νCC(38), βCD(28), βCC(17), νCO(14)
655	634	γCD(95)
623	627	γCD(72), γCC(16), γCO(12)
593	597	βCC(80), νCC(9)
551	552	γCC(64), γCD(34)
509	508	βCC(75), νCO(10), νCC(8)
432	435	γCD(39), γCC(31), γCO(29)
367	367	βCO(76), νCC(8), βCC(7)
358	358	γCC(76), γCD(24)
235	235	τOD(68), γCC(27), γCO(5)
203	203	γCC(64), τOD(32)

[a] Mean deviation: 7.05 cm^{-1} (0.64%)

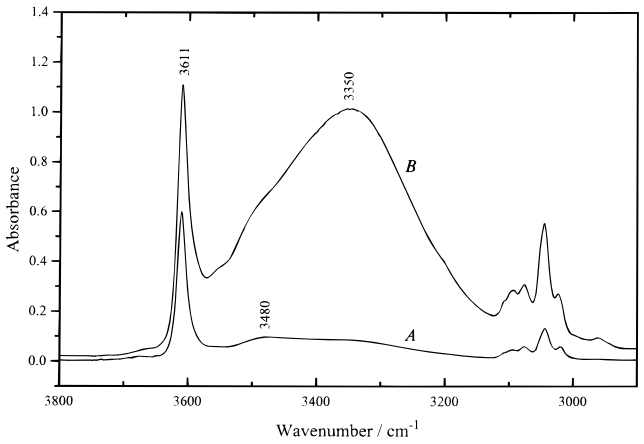

Figure 2. Effect of dilution on the infrared spectrum of the CCl_4 solution of phenol in the 3800−2900 cm^{-1} region (CCl_4 spectrum subtracted): A, 1% (m/m) solution (5x ordinate expansion); B, 5% (m/m) solution.

Comparing the spectra in the νCD−νOD and νCH−νOH region (Figure 5) a similar association pattern of the OD- and OH-groups is apparent (see the 2500−2600 cm^{-1} and the 3200−3600 cm^{-1} regions). When interpreting the spectra we had to keep in mind that our phenol-d_6 spectra contained bands of phenol-d_5 as well: the deuteration of the ring was practically complete, but only about 70% of the hydroxyl hydrogens were exchanged by deuterium.

C. Normal Coordinate and Intensity Calculations. The observed and calculated frequencies of C_6H_5OH, C_6H_5OD, C_6D_5OH, and C_6D_5OD are presented together with the potential

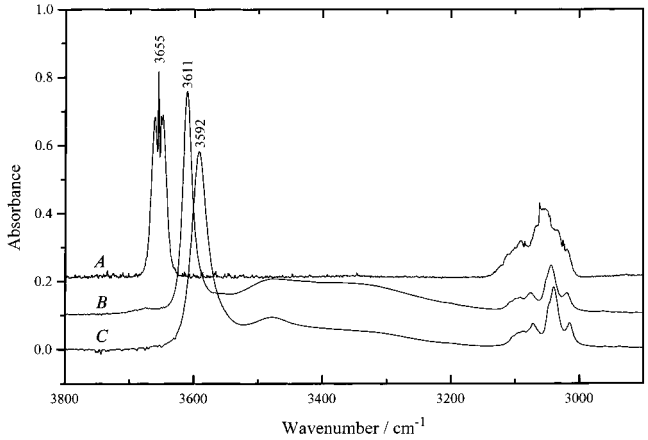

Figure 3. Solvent effect in the IR spectrum of phenol in the 3800−2900 cm^{-1} region: A, vapor spectrum; B, CCl_4 solution; C, CS_2 solution.

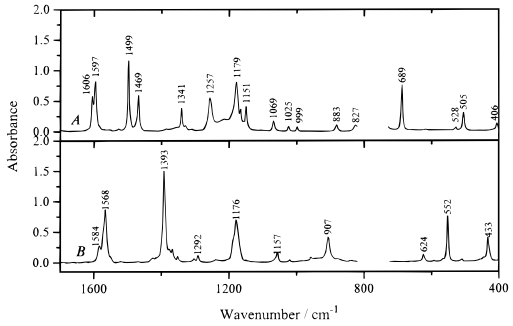

Figure 4. IR spectra of phenol (A) and hexadeuteriophenol (B) in the 17000−400 cm^{-1} region in CCl_4 solution.

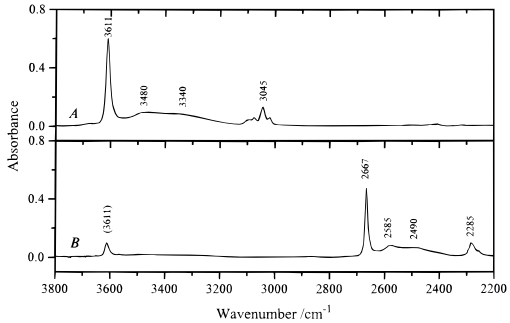

Figure 5. IR spectra of phenol (A) and hexadeuteriophenol (B) in the 3750−2200 cm^{-1} region in CCl_4 solution.

energy distributions for each normal mode in Tables 4, 5, 6, and 7, respectively. In case of the parent molecule the observed and calculated relative absorption intensities are also given in Table 4.

In spite of the fact that the optimization of the scale factors was based *only* on the C_6H_5OH frequencies, the resulting absolute and relative mean deviations between the measured and calculated frequencies of all the four isotopomers are similar and very small indeed, which is a good proof of the reliability of the force field.

Obviously, a shift of certain fundamental frequencies towards lower wavenumbers was expected on deuteration. The analysis of the eigenvectors and PEDs reveals some interesting details. As expected, the CH, CD, OH, and OD stretching vibrations have highly characteristic frequencies, since they are pure group vibrations. The CO stretching and OH bending coordinates, on the other hand, contribute considerably to more than one vibrations, and these contributions change substantially with the

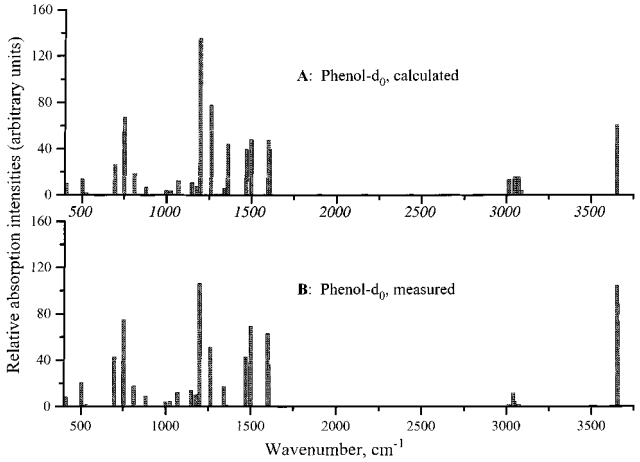

Figure 6. Comparison of the calculated (A) and measured (B, in solution) relative absorption intensity patterns of phenol (from data in Table 4).

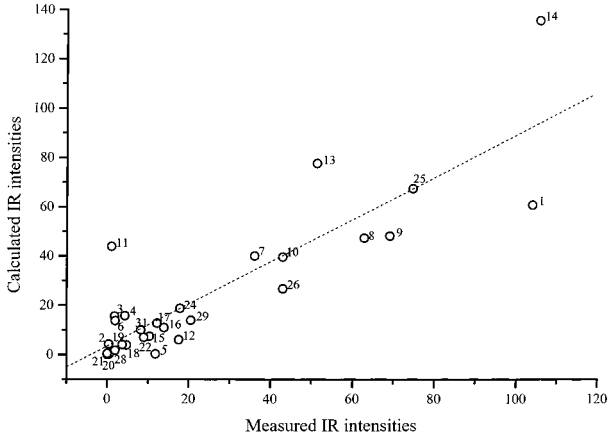

Figure 7. Calculated *vs.* measured relative absorption intensities of fundamental vibrational transitions of phenol (from data in Table 4).

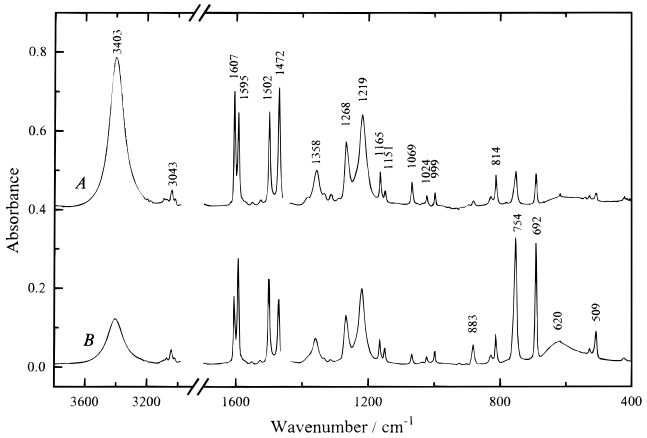

Figure 8. Polarized IR spectra of phenol aligned in a nematic solution (5% m/m) in ZLI-1695; uniaxial alignment, electric vector parallel (A), and perpendicular (B), with the director of the liquid crystalline sample.

extent of deuteration. The energy distribution of the CO stretching motion is not sensitive to O-deuteration but changes on deuteration of the ring. When the phenyl group is not deuterated, the ν_{13} normal mode with a frequency of about 1250−1260 cm^{-1} contains about 50% of νCO (according to the PED), while only 6% of νCO is found in higher frequency modes, which is the 1500 cm^{-1} vibration in phenol and phenol-OD. If, however, the phenyl group is fully deuterated (C_6D_5 group instead of C_6H_5), both frequencies concerned decrease by about 70 cm^{-1} and the contribution of the νCO coordinate increases in the higher frequency mode and decreases in the lower frequency mode.

In contrast, the OD bending vibration is more characteristic than is the OH bending vibration. There are rather pure OD in-plane bending characteristic frequencies with βOD participation of 65 and 78% in the spectra of C_6D_5OD and C_6H_5OD, respectively, while the highest contribution of the βOH coordinate to a normal coordinate is 45 and 38% in the case of C_6H_5-OH and C_6D_5OH, respectively.

The OH torsional vibrations are very characteristic: their PED is 97 and 96% in one normal coordinate of C_6H_5OH and C_6D_5-OH, respectively. In contrast, the OD torsional coordinate is distributed between two normal modes with the two lowest frequencies; it gets strongly coupled with an out-of-plane ring deformation vibration.

The calculation of IR intensities is known to be less successful than that of the frequencies. At this level of theory, however, there is a recognizable similarity between the calculated and observed intensity pattern of phenol-d_0 (see Figure 6), although the correlation shown in Figure7 is still not as good as would be desirable.

D. Linear Dichroism and Asymmetry of Molecular Dynamics. As we have seen above, even disregarding the H-atom of the O−H-group, the C_{2v} symmetry of the molecular skeleton in phenol is ruined. Concerning the vibrational assignment, the key question is whether these small distortions and the asymmetric influence of the OH bond are negligible with respect to the phenyl group vibrations so that they can be classified under the C_{2v} symmetry species, or are significant enough to defy such a description.

One way of answering this question is by inspecting the calculated normal modes to see whether they are symmetric or not. This, however, may be a tedious procedure; in addition, it would be hard to define a common limit of tolerance of asymmetry for different vibrations. Besides, it always remains a question how reliable our calculated eigenvectors are.

We consider it a more effective way to estimate the deviation of the dynamic properties of the molecule from symmetric behavior by examining the vibrational transition moment directions. This can be done both experimentally and theoretically, which provides a cross-checking possibility. When the symmetry is high enough, C_{2v} or higher, the transition moments are aligned along three mutually orthogonal axes within the molecule. When the symmetry is lower than that (i.e., C_{2h}, C_s, C_i, or C_1), the transition moments assume more than three different directions. In practice the simplest way may be to measure the linear dichroism of uniaxially oriented samples (solute molecules aligned in nematic liquid crystal or in stretched polymer) to determine the dichroic ratios of absorption bands, parameters that are dependent on the transition moment directions.

Out-of-plane Vibrations. The two basic polarized IR spectra of phenol in LC solution are shown in Figure 8. The dichroic ratios d_i determined as $d_i = I_p/I_s$ (i.e., as ratios of the band intensities measured at p (parallel) polarization to those at s (perpendicular) polarization) are given in the third column of Table 8. Note that the d_i values range from 0.325 to 3.71 but they assume *more than three* different values. The transition moments of the out-of-plane vibrations, being perpendicular to the plane of the molecule, are expected to be the least aligned along the direction of sample orientation (the director of the liquid crystal); thus, the smallest d_i values are expected to belong

TABLE 8: Dichroic Ratios (d_i), Orientation Factors (K_i), and Observed and Calculated Transition Moment Directions (ϕ_i^{exp} and ϕ_i^{calc}, Respectively) of Phenol-d_0

i	ν_i	d_i	K_i	ϕ_i^{exp}	ϕ_i^{calc}
1	3403	3.71	0.65	0.0	−0.6
2	3093	3.70	0.65	0.0	0.7
3	3074	0.92	0.32	60.7	73.8
4	3050	1.27	0.39	−50.5	−30.0
5	3043	1.27	0.39	−50.5	−21.1
6	3021	1.86	0.48	38.2	15.1
7	1607	2.00	0.50	35.7	26.1
8	1595	1.01	0.34	57.7	60.2
9	1502	1.18	0.37	52.8	47.9
10	1472	2.03	0.50	35.2	26.7
11	1358	1.57	0.44	43.7	38.7
12	1335	3.30	0.62	−14.4	−6.2
13	1268	1.40	0.41	47.4	38.3
14	1219	1.40	0.41	47.4	44.2
15	1165	1.46	0.42	46.0	26.6
16	1151	0.86	0.30	63.0	67.2
17	1069	2.41	0.55	−29.0	−12.7
18	1024	1.58	0.44	43.5	41.5
19	999	1.38	0.41	47.8	46.2
20	971	nmV[a]	nmV	nmV	*x*[b]
21	952	nmV	nmV	nmV	*x*
22	883	0.325	0.14	*x*	*x*
23	(829)	1.13	0.36	54.1	*x*
24	814	1.13	0.36	54.1	40.4
25	754	0.325	0.14	*x*	*x*
26	692	0.325	0.14	*x*	*x*
32	620	0.325	0.14	*x*	*x*
27	619	3.70	0.65	0.0	−78.3
28	529	0.79	0.28	65.9	55.7
29	509	0.325	0.14	*x*	*x*
30	(424)	1.05	0.34	56.5	*x*
31	415	2.00	0.50	35.7	38.4

[a] nmV = no measured value. [b] *x*: out-of-plane direction.

to the out-of-plane vibrations. This means that the observed dichroic ratios can be used, without any further manipulations, to check the assignment of the out-of-plane vibrations.

Indeed, data in Table 8 show that the strong bands at 754 and 692 cm^{-1} and the medium intensity bands at 883 and 509 cm^{-1} have this low dichroic ratio ($d_i = 0.325$) confirming that they belong to out-of-plane vibrations. Note that the broad absorption band at 620 cm^{-1} originating from τOH, the torsional vibration of the H-bonded OH-group, shows the same dichroic behavior as all out-of-plane vibrations. This can be regarded as a direct experimental evidence of the planar structure of phenol (at least in this solution), which agrees with the results of the quantum chemical calculations.

Our frequency calculations indicate that three more out-of-plane γCH bands should be found in the spectrum, two in the 950−980 cm^{-1} region and another one near 810−820 cm^{-1}. The first two bands can be seen in the CCl_4 solution spectrum (at 974 and 956 cm^{-1}) and even in the vapor spectrum (973 and probably 951 cm^{-1}), but they are too week to be studied in the LC solution spectrum (the weak features seen in the 900−990 cm^{-1} region in Figure 8 are artifacts due to imperfect compensation of the LC absorption bands). In the 800−830 cm^{-1} region there are two close-lying bands clearly observed in all phenol spectra; one of these has been assigned by all previous investigators to an in-plane vibration while the other to an out-of-plane vibration. According to our LD measurements, however, both bands have the same dichroic behavior with $d_i = 1.13$, differing very significantly from that of the out-of-plane bands. At the same time, we do not expect to have two in-plane fundamentals here either. The only interpretation consistent with all available data is that, on the one hand, the out-of-plane vibration in question is masked and too week to be observed (the ab initio calculated IR intensity of the ν_{23} vibration confirms this assumption, see Table 4), and on the other hand, the two bands with the same in-plane polarization are due to Fermi resonance of ν_{23} with $2\nu_{31}$ (2×410) = 820 cm^{-1}).

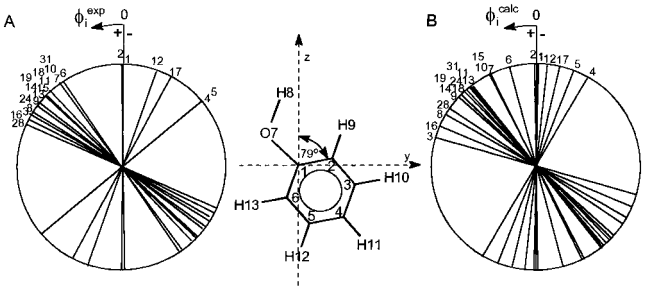

Figure 9. Comparison of measured (A) and computed (B) vibrational transition moment directions of phenol fundamentals (see data in Table 8).

In-Plane Vibrations. The bands corresponding to the in-plane vibrations have individual dichroic ratios ranging from 0.79 to 3.71, the highest d_i value being that of the OH stretching band (the very broad band centered at 3403 cm^{-1}). This indicates that the OH bonds of phenol molecules are oriented preferentially along the director of the liquid crystal, probably due to a nearly linear hydrogen bond formed with the nitril groups of the rodlike molecules of the LC material. For this reason the transition moment direction of the O−H stretching band was accepted as the axis of preferential orientation (the "long" axis, *z*) of phenol molecules.

To obtain the transition moment directions of other in-plane bands from the measured dichroic ratios, the method described by Michl and Thulstrup[19] was used. According to this, the orientation factors K_i were first calculated for each band as

$$K_i = d_i/(d_i + 2) \tag{1}$$

then the angles ϕ_i that the transition dipole moment of an in-plane vibration makes with the axis of preferential orientation *z* were obtained from the relation:

$$\tan^2 \phi_i = (K_z - K_i)/(K_i - K_y) \tag{2}$$

where $K_z = K_{\nu OH} = 0.65$, and $K_y = 0.21$, the orientation factor of the "short" in-plane axes, *y*; the latter was obtained from the condition $K_x + K_y + K_z = 1$, where $K_x = 0.14$ is the orientation factor of the out-of-plane *x* axis of the molecule.

Surprisingly, the computed transition moment direction of the νOH vibration makes an angle of nearly 38° with the OH bond direction according to our DFT/B3P86 calculation (see the *z*-axis in Figure 9). Nevertheless, this direction (rather than the direction of the O−H-bond) was accepted in the molecule-fixed coordinate system as the axis of preferential orientation of phenol molecules, and the angles ϕ_i were measured from this direction in anticlockwise sense within the plane of the molecule (Figure 9).

The frequencies observed in the LC solution, dichroic ratios, orientation factors, and transition moment directions determined both experimentally (ϕ_i^{exp}) and from the DFT calculation (ϕ_i^{calc}) are listed in Table 8.

Unfortunately, the sign of ϕ_i cannot be determined from eq 2, whereas there is no sign ambiguity in the theoretical calculation. Thus the signs of the calculated ϕ_i^{calc} values were accepted for those of the measured ϕ_i^{exp} values as well. For

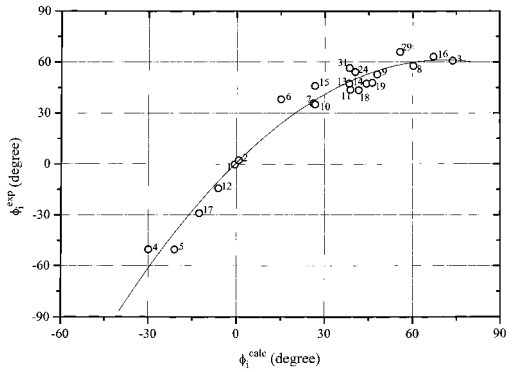

Figure 10. Plot of measured vs DFT calculated vibrational transition moment directions of phenol fundamentals (see data in Table 8).

the sake of easier comparison, the experimental and theoretical transition moment directions are presented also in graphical form in Figure 9A and B, respectively. The mean deviation between the pairs of corresponding values is not very small (10.2°), but at this stage we are unable to evaluate the relative errors of the two sets of values (i.e. it is not known which of them is closer to reality). Nevertheless, there are definite similarities between the two patterns.

(i) The transition moments are not grouped around two mutually perpendicular directions (as should be in a molecule having C_{2v} symmetry) but are scattered very strongly in a wide range of angles. The experimental and theoretical results also agree in that there is a rather large angle interval (more than 60°) where no transition moments have been found.

(ii) The sequence of vibrations indicated by the serial numbers of normal modes around the two circles in Figure 9 shows great similarities, too (i.e. there seems to be a definite correlation between the observed and calculated transition moment directions, which is depicted in Figure 10).

Unexpectedly, the data points in Figure 10 are best fitted with a second-order polynomial instead of a straight line. The reasons of the deviation of this correlation from linearity is the subject of further studies involving IR-LD studies of phenol-d_5 as well.[24]

All the above data and observations indicate that the overall picture of the strongly asymmetric distribution of transition moment directions must be essentially right. It allows to make the conclusion that the symmetry of molecular vibrations of phenol is C_s at most, and classification of the normal modes under C_{2v} symmetry species, even approximately, is not justified.

V. Conclusion

The molecular structure and vibrational assignment of phenol and its three main deuterated isotopomers have been re-examined with the use of new experimental data and DFT calculations. A planar structure with a distorted benzene ring has been obtained from both the quantum chemical calculations (for the free molecule) and infrared linear dichroism measurements (in LC solution).

The B3P86 method with the 6-311G** basis set gave us (after fitting a few scale factors) a reliable force field that proved to be transferable among the isotopomers for vibrational frequency calculations and assignments. This way we proposed a more reliable revised assignment of the vibrational spectra of phenol molecule, based on PED and supported by measured and calculated infrared absorption intensities and transition dipole moment directions. On the basis of the latter, we advocate that the symmetry of in-plane vibrations in phenol is reduced to such an extent that there are no real grounds to classify the normal modes under C_{2v} symmetry species.

Similar work to solve the assignment problems of polyhydroxy benzenes such as hydroquinone are in progress.[25] The application of the scale factors obtained for phenol seems to be feasible in these calculations.

Acknowledgment. This work has been supported by research grants T014479 (to G.K.), T014064 (to F.B.), and T015756 (to M.K.) from the Hungarian National Research Fund (OTKA) for which the authors are greatly indebted.

References and Notes

(1) Larsen, N. W. *J. Mol. Struct.* **1979**, *51*, 175.
(2) Portalone, G.; Schultz, Gy.; Domenicano, A.; Hargittai, I. *Chem. Phys Lett*. **1992**, *197*, 482.
(3) Konschin, H. *J. Mol. Struct*. **1983**, *92*, 173.
(4) Puebla, C.; Ha, T.-K. *J. Mol. Struct. (THEOCHEM)* **1990**, *204*, 337.
(5) Bock, C. W.; Trachtman, M.; George, P. *J. Mol. Struct. (THEOCHEM)* **1986**, *139*, 63.
(6) Bock, C. W.; Hargittai, I. *Struct. Chem*. **1994**, *5*, 307.
(7) Mecke, R.; Rossmy, G. *Z. Elektrochemie* **1955**, *59*, 866.
(8) Evans, J. C. *Spectrochim. Acta* **1960**, *16*, 1382.
(9) Green, J. H. S. *J. Chem. Soc*. **1961**, 2236.
(10) Bist, H. D.; Brand, J. D. C.; Williams, D. R. *J. Mol. Spectrosc.* **1966**, *21*, 766; *J. Mol. Spectrosc.* **1967**, *24*, 402.
(11) Varsányi, G. *The Assignment of Vibrational Spectra of 700 Benzene Derivatives*; Academic Press: Budapest, 1973; p 77.
(12) Larsen, N. W.; Nicolaisen, F. M. *J. Mol. Struct*. **1967**, *22*, 29.
(13) Hutt, K. W.; Butcher, R. J. *J. Phys. C: Solid State Phys.* **1988**, *21*, 6013.
(14) Wilson, H. W.; MacNamee, R. W.; Durig, J.R. *J. Raman Spectrosc.* **1981**, *11*, 252.
(15) Kovner, M. A.; Davydova, N. I.; Zhigunova, I. A. *Opt. Spektrosk.* **1965**,. *18*, 152.
(16) Sarin, V. N.; Rai, M. M.; Bist, H. D.; Khandelwal, D. P. *Chem. Phys. Lett*. **1970**, *6*, 473.
(17) Kubinyi, M.; Billes, F.; Grofcsik, A.; Keresztury, G. *J. Mol. Struct*. **1992**, *266*, 339.
(18) Belhakem, M.; Jordanov, B. *J. Mol. Struct.* **1990**, *218*, 309.
(19) Michl, J.; Thulstrup, E. W. *Spectroscopy with Polarized Light. Solute Alignment by Photoselection, in Liquid Crystals, Polymers, and Membranes*, VCH Publishers: New York, 1986; Chapter 5, pp 222−268.
(20) Becke, A.D. *J. Chem. Phys*. **1993**, *98*, 5648.
(21) Frisch, M. J.; Trucks, G. W.; Schlegel, H. B.; Gill, P. M. W.; Johnson, B. G.; Wong, M. W.; Foresman, J. B.; Robb, M. A.; Head-Gordon, M.; Replogle, E. S.; Gomperts, R.; Andres, J. L.; Raghavachari, K.; Binkley, J. S.; Gonzalez, C.; Martin, R. L.; Fox, D. J.; DeFrees, D. J.; Baker, J.; Stewart, J. J. P.; Pople, J. A. *Gaussian 92/DFT*, Revision F.3; Gaussian, Inc.: Pittsburgh, PA, 1993.
(22) Pulay, P.; Fogarasi, G.; Pang, F.; Boggs, J. E. *J. Am. Chem. Soc*. **1979**, *101*, 2550.
(23) Fogarasi, G.; Pulay, P. *J. Mol. Struct*. **1977**, *39*, 275.
(24) Keresztury, G.; Sundius, T. To be published.
(25) Billes, F.; Kubinyi, M. To be published.